Intestinal and Mucosal Microbiomic Response to Oral Challenge of Enterotoxigenic Escherichia Coli in Weaned Pigs

Shan-Shan Peng
Sun Yat-sen University
Yingjie Li
Sichuan Agricultural University
Qiuhong Chen
Sichuan Agricultural University
Qi Hu
the Neomics Institute
Ying He
Sichuan Agricultural University
Lianqiang Che
Sichuan Agricultural University
Ping-Ping Jiang (jiangpp3@mail.sysu.edu.cn)
Sun Yat-sen University

Research Article

Keywords: Infant diarrhoea, Enterotoxigenic Escherichia coli, Proteomics, Mucosal microbiome, Regularized Canonical Correlation Analysis, Bile acid

Posted Date: September 21st, 2021

DOI: https://doi.org/10.21203/rs.3.rs-888158/v1

Abstract

Enterotoxigenic Escherichia coli (ETEC) is closely associated with diarrhoea in children in resource-limited countries and of travellers' diarrhoea. This study aims to investigate the change of ileal mucosal microbiome and ileal protein expression as well as their correlation in pigs by *E. coli* K88 (ETEC). Seven weaned male pigs were orally given 1 ×10^9 CFU of ETEC (ETEC, n = 7), and the other seven received saline (CON, n = 7). Ileal tissues were obtained 48 h after the ETEC challenge for both proteomic and mucosal microbiomic analyses. Nine proteins were altered in expression level in the ETEC group, including decreased expression of FABP1 and FABP6 involved in bile acid circulation. TLR-9 mediated pathway was also affected at transcription level with increased expression of SIGIRR and MyD88. Correlation analysis revealed correlations between the ileal proteins and mucosal bacterial taxa, including the positive correlation between Lactobacilli and PPP3CA ($r = 0.9$, $p < 0.001$), and negative correlation between *Prevotella* with CTNND1 ($r = -0.7$, $p < 0.01$). In conclusion, ETEC infection caused inflammation and impaired the circulation of bile acids, and the mucosal microbiome may affect the expression of intestinal proteins. Further studies are needed for exact roles of these affected processes in the pathogenesis of ETEC-triggered diarrhoea.

Introduction

Enterotoxigenic *Escherichia coli* (ETEC) is a major cause of diarrhoea in children in resource-limited countries and of travellers' diarrhoea [1]. Diarrhoea is still one of the major causes of morbidity and mortality in children. Approximately 500,000 children died from diarrhoea in 2018, 20% of which happened in the second half-year of life [2-4].

ETEC adheres to the intestinal epithelial cells (IEC) in the jejunum and ileum through adhesins interacting with specific receptors and secrets enterotoxins to cause perturbation of hydroelectrolytic secretions resulting in a rapid onset of secretory diarrhoea leading to dehydration [5]. Despite the high prevalence of ETEC-associated diarrhoea, the detailed response of the gut to ETEC infection is yet fully understood. Multiple biological pathways and the gut microbiome have been found being involved in ETEC-triggered diarrhoea by *in vitro* [6,7] and *ex vivo* studies [8], and *in vivo* animal studies using pigs [9] and mice[10], including innate immunity response involving nuclear factor-κB (NF-κB) and mitogen-activated protein kinase (MAPK) pathways, intestinal barrier function involving tight junction proteins, intestinal ion transporters and water channel. Previous studies mainly focused on the intestinal response in the jejunal segment leaving that of the ileal segment less characterised. The askew gut microbiome has been associated with diarrhoea. Intervention using probiotics, such as Lactobacilli [6,7] or *Saccharomyces cerevisiae* [11] ameliorating diarrhoea, also highlights the involvement of the gut microbiome in ETEC-associated diarrhoea. Since altered gut microbiome was also found in osmotic diarrhoea, the relationship between the changed gut microbiota and infectious diarrhoea remains unclear and it could be diarrhoea and/or ETEC infection that change the gut microbiome. Currently available studies were mainly on the cecum [12], jejunal digesta and faeces [13] of ETEC-treated animals. It is of interest to know how the

mucosal microbiome in the small intestine is changed post the ETEC infection given ETEC attaches to the intestine mucosa.

Here in this study changes of ileal proteins and the mucosal microbiome in the ileum post ETEC challenge in weaned pigs were profiled by untargeted proteomics and 16S amplicon sequencing, respectively. Further correlation analysis was also conducted to explore the potential association between intestinal proteins and bacterial taxa.

Materials And Methods

Animal Procedure and Sample Collection

The animal experiment was carried out in accordance with the guidelines and regulations of the Animal Care and Ethical Committee of the Sichuan Agricultural University and was in compliance with the ARRIVE guidelines. The ethical approval for the animal procedure was granted by the Animal Care and Use Committee of the Sichuan Agricultural University (SCAUAC-20200051).

After acclimatisation for a week, 14 male weaned pigs aged 28 d (Duroc × Landrace × Yorkshire) were randomly allocated into two groups, the group challenged by enterotoxigenic *Escherichia coli* K88 (the ETEC group, n = 7) and the unchallenged group (the CON group, n = 7). The inoculum for the ETEC group is Luria Broth containing ETEC (100 mL, 1×10^9 CFU/mL, serotype O149: K91: K88ac; China Veterinary Culture Collection Centre, Wuhan, China), and the CON group received 100 mL sterilised Luria broth. The two groups were reared on the same diet and water *ad libitum*, kept in separate rooms to avoid cross contamination at controlled temperature (28-30˚C). The ingredient composition and nutrient levels of the diet are presented in **Table S1**.

Self-defined diarrhoea scores (1, normal; 2, pasty; 3, semi-liquid; 4, watery) were recorded at 0, 4, 8, 16, 20, 24, 30 and 36 hs after the ETEC challenge. All pigs were euthanized with an intramuscular injection of 15 mg/kg body weight of pentobarbital sodium under anaesthesia 48 h after the ETEC challenge. Two sections of ileal tissue (2 cm in length) were collected from each pig with one stored in 4% paraformaldehyde solution for histology and the other snap-frozen and stored at -80 °C for proteomic and transcription analyses.

Intestinal Morphology

Ileal tissues were cross sectioned and stained with the periodic acid Schiff method (PAS staining). Ten villi and crypts of each section were measured (Image ProPlus 6.0, company, city, country) under a microscope and the villi-crypt ratio (VCR) was calculated.

Proteomics of the Ileal Tissues

The ileal samples were processed according to the enhanced filter-aided sample preparation (eFASP) protocol [48]. Briefly, frozen tissue samples were homogenised using a TissueLyser II (Qiagen,

Gaithersburg, MD, USA) in a lysis buffer containing 4% sodium dodecyl sulphate, 0.2% deoxycholic acid, 50 mmol/L dithiothreitol and 100 mmol/L ammonium bicarbonate (pH 8.0). The lysate was incubated at 95˚C for 5 min and centrifuged (16,000 × g, 4˚C, 20min). Protein concentration of the obtained supernatant was determined by a BCA protein quantification kit (Thermo Scientific, Waltham, MA, USA). Supernatant containing 100 µg protein was transferred onto a centrifugal filter (Amicon Ultra, 10 kDa, Millipore, Darmstadt, Germany) and washed twice by mixing with an exchange buffer (8 mol/L urea, 0.2% deoxycholic acid, 100 mmol/L ammonium bicarbonate, pH 8.0) followed by a centrifugation (14,000 × g, 15 min). The protein was reduced by Tris(2-carboxyethyl)phosphine (TCEP, 0.01 mol/L, 1:50 [v/v]), alkylated with iodoacetamide and digested by trypsin (1 µg/100 µg protein, Promega, Madison, WI, USA). Tryptic peptides were recovered and purified by phase extraction using ethyl acetate acidified by formic acid (1%, v/v). Vacuum-dried tryptic peptides were resuspended in 2% acetonitrile with 0.1% formic acid and applied onto a Dionex RSLC UPLC System (Thermo Scientific) coupled to an Orbitrap Fusion Lumos Mass Spectrometer (Thermo Scientific). One µg of peptide was injected onto a 2 cm C18 material-trapping column and separated on an analytical column (Acclaim PepMap100, 75 µm ID, 15 cm, 100 Å, Thermo Scientific) with both columns kept at 40˚C. The peptides were eluted at a stable flow rate of 300 nL/min with a linear gradient from a solution of 2.4% acetonitrile and 0.1% formic acid to a solution of 78% acetonitrile and 0.1% formic acid in 150 min. Mass spectrometric data were obtained in the positive ionization mode in a data-dependent acquisition (DDA) mode. The mass spectra are available at the ProteomeXchange Consortium (proteomexchange.org) with the data set identifier PXD028066.

Protein annotation and quantification were carried out using MaxQuant (version 1.5.2.8) [49] against the Uniprot database (*Sus scrofa*, UP000008227, last modified 2021-01-29). Detection of at least two unique peptides per protein and protein being present in at least 50% of the samples in each group were required. Protein abundance data were normalized and two-based logarithm transformed using the Perseus software (version 1.6.5.0) [50] before data analysis.

RT-qPCR of Ileal Genes

Transcription levels of selected genes in the ileum were tested by quantitative RT-qPCR using predesigned primers (**Table S3**). Briefly, tissue RNA was extracted using Trizol Reagent (TaKaRa Biotechnology, Dalian, China) according to the manufacturer's instructions. The reverse transcription was performed using a cDNA reverse transcription kit (Vazyme Biotechnology, Nanjing, China) and the obtained cDNA was amplified with a SYBR green kit (Vazyme Biotechnology, Nanjing, China) on an ABI-7900HT Fast Real-Time PCR System (Applied Biosystems, Foster City, CA, USA). The transcription levels of target genes were normalised to the housekeeping gene, ACTB, and analysed using the $2^{-\Delta\Delta Ct}$ method [51].

Full-Length 16S Sequencing of the ileal mucosal microbiome

The full-length 16S sequencing of the ileal mucosal microbiome was performed as previously described [52]. Briefly, the ileal mucus was scraped and the bacterial genomic DNA was extracted with a DNA Stool Mini-Kit (QIAGEN, Hilden, Germany). The DNA concentration was estimated on a NanoDrop

spectrophotometer (Thermo Scientific). The 16S rRNA gene was amplified by PCR with specific primers. The DNA libraries were constructed on the amplicons with the SMRT Bell technology on a PacBio RS II sequencer (Pacific Biosciences, Menlo Park, CA, USA) [53]. The raw reads were processed using Lima software (version 1.11.0) to obtain circular consensus sequence (CCS) reads. Further sample sorting, trimming, clustering of OTUs were conducted with the USEARCH software [54].

Data Analysis

All data analysis were conducted in R [55] integrated with R Studio [56]. Body weight, diarrhoea score, intestinal morphology and transcription levels of ileal genes were analysed by student's *t* test or Wilcoxon sum-rank test.

The proteomic data were firstly analysed with a semi multivariate method, the NSC analysis to locate proteins associated with the ETEC challenge using the package *pamr* in R [57]. The mount of shrinkage value was determined using a 5-fold cross validation, and the NSC probability analysis with a probability cut-off of 90%. Proteins selected with differentiating power by NSC were further verified by Student's *t* test or Chi-squared test. A protein with a p value < 0.05 and absolute effect size > 0.8 was regarded as significantly different between the treatment groups.

For the mucosal microbiomic analysis, OTUs present in at least 50% of all samples or higher than 75% of all counts were selected and a total of 111 were selected out. OTU information and abundance were aligned with treatment groups for data analysis in R. Alpha-diversity shown as Shannon index was calculated and compared between the treatment groups. Beta-diversities based on the unifrac and weighted unifrac distances were tested by permutation test and presented in PCoA plots. Wilcoxon sum-rank test was used to analyse taxon abundance between the treatment groups.

Correlation Analysis of The Microbiomic and Proteomic Data

Correlation between the mucosal microbiomic and proteomic data was firstly conducted by a multivariate correlation analysis, rCCA, with the R package *mixOmics* [58]. The regularising λs for the two datasets were obtained by permutation. Any correlation with the correlation product > 1.0 was selected and were further verified with Spearman correlation analysis. Only the correlations with $p < 0.05$ and correlation coefficient (ρ) > 0.8 were presented.

Results

Fourteen weaned male pigs (aged 28 d) were randomly allocated into two groups, one received ETEC challenge (the ETEC group, n = 7) and the other received sterile carrier as the CON group (n = 7).

Body Weights, Diarrhoea Scores and Ileal Morphology

The diarrhoea scores over the time post the ETEC challenge were showed in **Figure 1,** the difference of the diarrhoea scores between two groups peaked at 16 hrs. At 36 hrs post the challenge, the diarrhoea scores in the ETEC group were close to those in the CON group. No significant difference was observed in the body weight between the ETEC and CON pigs at euthanasia ($p > 0.05$). No significant difference was observed in intestinal morphological parameters, the villous height, the crypt depth or the ratio of villous height over crypt depth, in the ileum between the two treatment groups ($p > 0.05$). The body weight at euthanasia and the intestinal morphological parameters were presented in **Table S2**.

Ileal Proteomics

In total, 5151 ileal proteins were annotated, and 47 proteins were selected by the semi-multivariate analysis, Nearest Shrunken Centroid (NSC) analysis, as being able to differentiate the two treatment groups. Nine proteins had significantly different abundance between the ETEC and CON pigs ($p < 0.05$, |effect size| > 0.80) as further verified by the Student's *t*-test. Information of these proteins, including accession number, protein name, gene name, biological process, abundance in the two treatment groups, p value and effect size was listed in **Table 1**. Four proteins showed decreased expression in the ETEC pigs, relative to the CON ones, including Fatty acid binding proteins 6 (FABP6, the ileal form) and 1 (FABP1, the liver form), ADP ribosylation factor like GTPase 8B (ARL8B) and Cytochrome C oxidase subunit (COX6A1). FABP6 and 1, and COX6A1 are involved in metabolism of bile acids and energy, whilst ARL8B is involved in antigen presentation. Among the five proteins showed increased expression in the ETEC pigs, are involved in immune response, metabolism of nuclear acid and protein and cell cycle regulation.

Transcription of Selected Genes in the Ileums

To extend the findings by proteins findings, a group of selected genes were tested by RT-qPCR. Transcription levels of ASBT ($p < 0.01$) and IL-18 ($p < 0.05$) decreased, whilst those of TLR9 ($p < 0.01$), MyD88 ($p = 0.05$) and SIGIRR ($p = 0.07$) increased in the ETEC pigs, relative to the CON ones (**Figure 2**). Transcription of gene, HIF (hypoxia-induced factor), was also documented, but was used for later correlation analysis.

Mucosal Microbiomics

In total, 447 operating taxonomy units (OTUs) were detected. Proteobacteria and Firmicutes were the two major phyla, followed by Bacteroidetes. The Bacteroidetes: Firmicutes ratios were 0.61 and 0.54 in the ETEC and CON pigs, respectively, but no significant difference was found between the two groups. The relative richness, the alpha diversity evaluated by the Shannon diversity index and beta diversity with unifrac distance at the genus level were shown in **Figure 3**. No significant difference ($p > 0.05$) was found in the alpha diversity (Wilcoxon rank-sum test, **Figure 3B**) or beta diversity (Adonis permutation test, **Figure 3C**) between the ETEC and CON groups. A genus from the order Rhizobiales showed significantly increased levels ($p < 0.05$, |effect size| = 0.62, Wilcoxon rank-sum test) in the ETEC pigs, relative to the CON ones. Two unassigned genera from the families Pirellulaceae ($p = 0.05$, |effect size| = 0.62) and

Enterobacteriaceae (p = 0.10, |effect size| = 0.62) showed trends of increase and decrease in the ETEC group, respectively.

Correlation of the Mucosal Microbiome and Intestinal Proteome

Regularized canonical correlation analysis (rCCA) [14] was used to explore correlations between the proteomic (proteins) and microbiomic (bacterial genera) data. rCCA-selected potential correlations were further verified by Spearman's correlation analysis. Correlations of these proteins and bacterial genera ($p < 0.05$, r = 0.8) were presented in **Figure 4**. The genus *Lactobacillus* was positively correlated with calcineurin A (PPP3CA, r = 0.9, **Figure 4B**). A negative correlation was observed between the genus *Prevotella* and catenin δ1 (CTNND1, r = -0.7, **Figure 4C**). An unclassified genus of the family Enterobacteriaceae was negatively correlated with tyrosine-protein kinase Lyn (r = -0.9, **Figure 4D**).

Discussion

In this study the ileal proteomic and mucosal microbiomic response to the oral challenge of ETEC were documented. As revealed by the proteomics analysis, ileal proteins involved in various biological functions were differentially regulated in the ETEC pigs, including the proteins related to immunity and infection, as well as the decreased proteins expression related to metabolism of bile acid and energy.

Among these proteins, proteins involved in bile acid transport, such as FABP6 and ASBT, showed the decreasing expression in the ETEC pigs. Bile acid transport is of pivotal importance in the metabolism of lipids. FABP6, mainly expressed in the ileum, transports bile acids in the epithelial cells to the basolateral domains and exit the epithelial cells [15]. Similarly, lowered ileal expression of FABP6 was also found in the pigs orally infected by *Salmonella typhimurium* [16], suggesting the involvement of bile acids metabolism in the bacterial diarrhoea. In the enterohepatic recycle of bile acids, more than 95% of the bile acids are reabsorbed in the ileum and transported back to the liver for reuse [17,18]. Apical sodium dependent bile acid transporter (ASBT), almost exclusively expressed in the ileum, is the main transporter that absorbs bile acids from the intestinal lumen [19]. Non-synonymous substitutions in ASBT amino acid sequence causes bile acid malabsorption and is associated with diarrhoea [20]. *In vitro* studies showed that challenge with *E. coli* significantly decreased the expression of ASBT in Caco2 cells [21]. Lack of ASBT results in faecal excretion of bile acids [22]. Bile acids entering enterocytes assisted by ASBT activate farnesoid X receptor (FXR), which activates FABP6 [23]. As reported, the decreased expression of ASBT and FABP6 can be attributed to the early inflammatory response impairing normal bile absorption in the ileum [24]. Therefore, the lower expressions of ASBT and FABP6 in this study suggest an accumulation of bile acids in the intestinal lumen, which is toxic to enterocytes. However, no luminal samples having been collected leaves us impossible to assess the bile acids levels in the digesta.

ETEC-induced diarrhoea involves mucosal inflammation, which is at least partly mediated by TLRs in murine [10] and pig models [25]. In our study, only TLR9 was increased in the ETEC pigs, which led to up-regulated transcription of MyD88 (myeloid differentiation factor 88), SIGIRR (single immunoglobulin

domain-containing IL1R-related) and down-regulated transcription of IL-18, which is in accordance with previous studies [26,27]. TLR9 recognises unmethylated CpG dinucleotides presented in the bacterial DNA and triggers downstream signal pathway, leading to elevated mucosal inflammation [28,29]. Up-regulation of downstream MyD88 and SIGIRR indicated the activation of this pathway [30]. However, activation of TLR9 on the apical/luminal surface of enterocytes can also inhibit NF-κB signalling, leading to tolerance of stimulation of TLRs, including TLR2 and TLR4 [31]. This may have contributed to the unchanged transcription of TLR2 and 4 detected here in this study (data not shown). Further investigation is needed on the cross-talk between different types of cells of the intestine under ETEC challenge. Of note, pro-inflammatory IL-18 does not only play part in the mucosal inflammation triggered by ETEC challenge, but also is involved in the maintenance of the intestinal barrier [32]. Decreased transcription of IL-18 observed here may have contributed to the impaired intestinal barrier frequently observed in the ETEC-challenged pigs.

It has been suggested that ETEC-induced diarrhoea is associated with an askew gut microbiome, which, not the ETEC per se, triggers the diarrhoeal symptoms [13]. ETEC attaches to the intestinal tissue by its adhesins that promote binding and colonization of the intestinal epithelium and enterotoxins responsible for triggering inflammation and fluid secretion [33]. A few studies have documented the changes of the faecal or digesta microbiome in ETEC-treated pigs [34–36]. In this study, the mucosal microbiome, instead of the luminal or faecal microbiome, was profiled by directly analysing the ileal tissues with luminal content emptied. About 80% of the bacteria in the mucosal microbiome detected belong to Proteobacteria and Firmicutes phyla, which is similar to previous studies on the digesta or faecal microbiome [13]. An increased Bacteroidetes: Firmicutes ratio was found in the ETEC pigs, which was different from previous study on pig model and humans with travellers' diarrhoea [13,37]. In a previous study effects of on ETEC on the microbiome of ileal digesta, but not on that of faeces, were observed in both community richness and diversity on day 9 post inoculation [36]. In this study, however, no significant difference was observed in relative abundance between the two treatment groups, which indicates the mucosal microbiome was relatively stable when pigs received ETEC challenge. The exact roles of the mucosal and digesta (luminal) microbiome in response to ETEC infection warrant further studies.

The rCCA applied in this study was adopted to reveal potential correlations between the intestinal proteins and mucosal bacterial taxa. The positive correlation between Lactobacilli and PPP3CA suggests a potential role of Lactobacilli in regulating the intestinal function, as PPP3CA induces of transcription of HIF-1α [38], which can alleviate local inflammation and maintains the intestinal barrier through the induction of intestinal trefoil factor (ITF) and Ecto-5´-nucleotidase (CD73)[39–41]. Similar to our findings, *Lactobacillus* was found associated with HIF-responsive ITF in a mouse model [42]. Faecal levels of the genus of *Prevotella* was found negatively associated with diarrhoea [43], though *Prevotella* stimulates epithelial cells to produce cytokines and promotes Th17-mediated inflammation and neutrophil recruitment [44]. CTNND1 regulates cell-cell adhesion [45]. The negative correlation found in our study suggested that mucosal *Prevotella* may affect the intestinal inflammation partially through the regulation

of CTNND1. Lyn is a member of Src family kinases (SFK) regulating the response of immune cells, such as B cells and mast cells, and promotes the production of immune factors [46]. Studies have shown that bacteria from the family Enterobacteriaceae, such as *Citrobacter rodentium* and *Salmonella entericaare*, could affect expression of Lyn [47]. Due to the limits of the sequencing technology adopted, the exact genus correlated with Lyn in ileum was unknown and further experiments are needed.

Conclusions

The oral infection of ETEC affected ileal proteins involved in various biological functions, such as bile acid metabolism and the NF-κB pathway using weaned pig as model. The impact of ETEC infection on mucosal microbiome in the ileum was limited, but the correlation of bacteria to ileal protein expression was observed. Further studies are needed to verify our findings about the underlying mechanism in the pathogenesis of ETEC-triggered diarrhoea.

Declarations

Author Contributions statement

S.S.P. wrote the manuscript and analyzed the data. S.S.P., Y.J.L., Q.H.C. and Y.H conducted the experiments. Q.H and P.P.J analyzed the data. L.Q.C and P.P.J conceived the experiments. P.P.J reviewed and edited the manuscript. All authors have read and agreed to the published version of the manuscript.

Funding

This work was supported by a start-up grant from Sun Yat-sen University, China to PPJ (2017181).

Competing Interests

The authors declare no conflict of interest.

Data Availability

The data presented in this study are available on request from the corresponding author.

Institutional Review Board Statement

Ethical approval was granted by the Animal Care and Use Committee of the Sichuan Agricultural University, Chengdu, China with the approval number as SCAUAC-20200051.

References

1. Porter, C. K. *et al.* A systematic review of experimental infections with enterotoxigenic *Escherichia coli* (ETEC). *Vaccine***29**, 5869–5885, doi:10.1016/j.vaccine.2011.05.021 (2011).

2. Youmans, B. P. *et al.* Characterization of the human gut microbiome during travelers' diarrhea., **6**, 110–119 https://doi.org/10.1080/19490976.2015.1019693 (2015).
3. Liu, Y. V. *et al.* Calcineurin promotes hypoxia-inducible factor 1alpha expression by dephosphorylating RACK1 and blocking RACK1 dimerization. *J Biol Chem*, **282**, 37064–37073 https://doi.org/10.1074/jbc.M705015200 (2007).
4. Louis, N. A. *et al.* Selective induction of mucin-3 by hypoxia in intestinal epithelia. *J Cell Biochem*, **99**, 1616–1627 https://doi.org/10.1002/jcb.20947 (2006).
5. Furuta, G. T. *et al.* Hypoxia-inducible factor 1-dependent induction of intestinal trefoil factor protects barrier function during hypoxia. *J Exp Med*, **193**, 1027–1034 https://doi.org/10.1084/jem.193.9.1027 (2001).
6. Louis, N. A. *et al.* Control of IFN-alphaA by CD73: implications for mucosal inflammation. *J Immunol*, **180**, 4246–4255 https://doi.org/10.4049/jimmunol.180.6.4246 (2008).
7. Wang, Y. *et al.* Lactobacillus rhamnosus GG treatment potentiates intestinal hypoxia-inducible factor, promotes intestinal integrity and ameliorates alcohol-induced liver injury. *Am J Pathol*, **179**, 2866–2875 https://doi.org/10.1016/j.ajpath.2011.08.039 (2011).
8. Bin, P. *et al.* Intestinal microbiota mediates Enterotoxigenic Escherichia coli-induced diarrhea in piglets. *BMC Veterinary Research*, **14**, 385 https://doi.org/10.1186/s12917-018-1704-9 (2018).
9. Larsen, J. M. The immune response to Prevotella bacteria in chronic inflammatory disease., **151**, 363–374 https://doi.org/10.1111/imm.12760 (2017).
10. Smalley-Freed, W. G. *et al.* p120-catenin is essential for maintenance of barrier function and intestinal homeostasis in mice. *J Clin Invest*, **120**, 1824–1835 https://doi.org/10.1172/jci41414 (2010).
11. Ingley, E. Functions of the Lyn tyrosine kinase in health and disease. *Cell Communication and Signaling*, **10**, 21 https://doi.org/10.1186/1478-811X-10-21 (2012).
12. Roberts, M. E. *et al.* Lyn Deficiency Leads to Increased Microbiota-Dependent Intestinal Inflammation and Susceptibility to Enteric Pathogens. *The Journal of Immunology*, **193**, 5249 https://doi.org/10.4049/jimmunol.1302832 (2014).
13. Erde, J., Loo, R. R., Loo, J. A. & Enhanced FASP (eFASP) to increase proteome coverage and sample recovery for quantitative proteomic experiments. *J Proteome Res*, **13**, 1885–1895 https://doi.org/10.1021/pr4010019 (2014).
14. Cox, J. & Mann, M. MaxQuant enables high peptide identification rates, individualized p.p.b.-range mass accuracies and proteome-wide protein quantification. *Nat Biotechnol*, **26**, 1367–1372 https://doi.org/10.1038/nbt.1511 (2008).
15. Tyanova, S. *et al.* The Perseus computational platform for comprehensive analysis of (prote)omics data. *Nat Methods*, **13**, 731–740 https://doi.org/10.1038/nmeth.3901 (2016).
16. Livak, K. J. & Schmittgen, T. D. Analysis of relative gene expression data using real-time quantitative PCR and the 2(-Delta Delta C(T)) Method., **25**, 402–408 https://doi.org/10.1006/meth.2001.1262 (2001).

17. Chen, P. *et al.* Modulation of gut mucosal microbiota as a mechanism of probiotics-based adjunctive therapy for ulcerative colitis. *Microb Biotechnol*, **13**, 2032–2043 https://doi.org/10.1111/1751-7915.13661 (2020).
18. Mosher, J. J., Bernberg, E. L., Shevchenko, O., Kan, J. & Kaplan, L. A. Efficacy of a 3rd generation high-throughput sequencing platform for analyses of 16S rRNA genes from environmental samples. *J Microbiol Methods*, **95**, 175–181 https://doi.org/10.1016/j.mimet.2013.08.009 (2013).
19. Edgar, R. C. Search and clustering orders of magnitude faster than BLAST., **26**, 2460–2461 https://doi.org/10.1093/bioinformatics/btq461 (2010).
20. CoreTeam, R. R. A Language and Environment for Statistical Computing.. R Foundation for Statistical Computing, Vienna.(2013).
21. Studio, R. S. T. R. Integrated Development for R. Boston, MA:RStudio, Inc.(2012).
22. pamr: Pam, prediction analysis for microarrays v. 1.56.1. (2018).
23. KA, L. C., González, I. & Déjean, S. integrOmics: an R package to unravel relationships between two omics datasets., **25**, 2855–2856 https://doi.org/10.1093/bioinformatics/btp515 (2009).
24. Uribe, J. H. *et al.* Transcriptional analysis of porcine intestinal mucosa infected with Salmonella Typhimurium revealed a massive inflammatory response and disruption of bile acid absorption in ileum. *Vet Res***47**, 11, doi:10.1186/s13567-015-0286-9 (2016).
25. Yi, Q. *et al.* Anethole Attenuates Enterotoxigenic Escherichia coli-Induced Intestinal Barrier Disruption and Intestinal Inflammation via Modification of TLR Signaling and Intestinal Microbiota. *Front. Microbiol.***12**, 647242, doi:10.3389/fmicb.2021.647242 (2021).
26. Li, X. Q. *et al.* Risks associated with high-dose Lactobacillus rhamnosus in an Escherichia coli model of piglet diarrhoea: intestinal microbiota and immune imbalances. *PLoS One***7**, e40666, doi:10.1371/journal.pone.0040666 (2012).
27. Peng, X. *et al.* Enterococcus faecium NCIMB 10415 administration improves the intestinal health and immunity in neonatal piglets infected by enterotoxigenic Escherichia coli K88. *J Anim Sci Biotechnol***10**, 72, doi:10.1186/s40104-019-0376-z (2019).
28. Kawai, T. & Akira, S. Signaling to NF-kappaB by Toll-like receptors. *Trends Mol Med***13**, 460–469, doi:10.1016/j.molmed.2007.09.002 (2007).
29. Blasius, A. L. & Beutler, B. Intracellular toll-like receptors. *Immunity***32**, 305–315, doi:10.1016/j.immuni.2010.03.012 (2010).
30. Yap, Y. A. & Mariño, E. An Insight Into the Intestinal Web of Mucosal Immunity, Microbiota, and Diet in Inflammation. *Front Immunol***9**, 2617, doi:10.3389/fimmu.2018.02617 (2018).
31. Lee, J. *et al.* Maintenance of colonic homeostasis by distinctive apical TLR9 signalling in intestinal epithelial cells. *Nature Cell Biology***8**, 1327–1336, doi:10.1038/ncb1500 (2006).
32. Nowarski, R. *et al.* Epithelial IL-18 Equilibrium Controls Barrier Function in Colitis. *Cell***163**, 1444–1456, doi:10.1016/j.cell.2015.10.072 (2015).

33. Dubreuil, J. D., Isaacson, R. E. & Schifferli, D. M. Animal Enterotoxigenic < i > Escherichia coli</i>. *EcoSal Plus***7**, ecosalplus.ESP-0006-2016, doi:10.1128/ecosalplus.ESP-0006-2016 (2016).
34. Li, Q. *et al.* Dietary Soluble and Insoluble Fiber With or Without Enzymes Altered the Intestinal Microbiota in Weaned Pigs Challenged With Enterotoxigenic E. coli F18. *Front. Microbiol.***11**, 1110, doi:10.3389/fmicb.2020.01110 (2020).
35. Wang, T. *et al.* Lactobacillus reuteri HCM2 protects mice against Enterotoxigenic Escherichia coli through modulation of gut microbiota. *Scientific Reports***8**, 17485, doi:10.1038/s41598-018-35702-y (2018).
36. Pollock, J., Hutchings, M. R., Hutchings, K. E. K., Gally, D. L. & Houdijk, J. G. M. Changes in the Ileal, but Not Fecal, Microbiome in Response to Increased Dietary Protein Level and Enterotoxigenic < i > Escherichia coli</i > Exposure in Pigs. *Appl Environ Microbiol***85**, doi:10.1128/AEM.01252-19 (2019).
37. Youmans, B. P. *et al.* Characterization of the human gut microbiome during travelers' diarrhea. *Gut Microbes***6**, 110–119, doi:10.1080/19490976.2015.1019693 (2015).
38. Liu, Y. V. *et al.* Calcineurin promotes hypoxia-inducible factor 1alpha expression by dephosphorylating RACK1 and blocking RACK1 dimerization. *J Biol Chem***282**, 37064–37073, doi:10.1074/jbc.M705015200 (2007).
39. Louis, N. A. *et al.* Selective induction of mucin-3 by hypoxia in intestinal epithelia. *J Cell Biochem***99**, 1616–1627, doi:10.1002/jcb.20947 (2006).
40. Furuta, G. T. *et al.* Hypoxia-inducible factor 1-dependent induction of intestinal trefoil factor protects barrier function during hypoxia. *J Exp Med***193**, 1027–1034, doi:10.1084/jem.193.9.1027 (2001).
41. Louis, N. A. *et al.* Control of IFN-alphaA by CD73: implications for mucosal inflammation. *J Immunol***180**, 4246–4255, doi:10.4049/jimmunol.180.6.4246 (2008).
42. Wang, Y. *et al.* Lactobacillus rhamnosus GG treatment potentiates intestinal hypoxia-inducible factor, promotes intestinal integrity and ameliorates alcohol-induced liver injury. *Am J Pathol***179**, 2866–2875, doi:10.1016/j.ajpath.2011.08.039 (2011).
43. Bin, P. *et al.* Intestinal microbiota mediates Enterotoxigenic Escherichia coli-induced diarrhea in piglets. *BMC Veterinary Research***14**, 385, doi:10.1186/s12917-018-1704-9 (2018).
44. Larsen, J. M. The immune response to Prevotella bacteria in chronic inflammatory disease. *Immunology***151**, 363–374, doi:10.1111/imm.12760 (2017).
45. Smalley-Freed, W. G. *et al.* p120-catenin is essential for maintenance of barrier function and intestinal homeostasis in mice. *J Clin Invest***120**, 1824–1835, doi:10.1172/jci41414 (2010).
46. Ingley, E. Functions of the Lyn tyrosine kinase in health and disease. *Cell Communication and Signaling***10**, 21, doi:10.1186/1478-811X-10-21 (2012).
47. Roberts, M. E. *et al.* Lyn Deficiency Leads to Increased Microbiota-Dependent Intestinal Inflammation and Susceptibility to Enteric Pathogens. *The Journal of Immunology***193**, 5249, doi:10.4049/jimmunol.1302832 (2014).

48. Erde, J., Loo, R. R. & Loo, J. A. Enhanced FASP (eFASP) to increase proteome coverage and sample recovery for quantitative proteomic experiments. *J Proteome Res* **13**, 1885–1895, doi:10.1021/pr4010019 (2014).
49. Cox, J. & Mann, M. MaxQuant enables high peptide identification rates, individualized p.p.b.-range mass accuracies and proteome-wide protein quantification. *Nat Biotechnol* **26**, 1367–1372, doi:10.1038/nbt.1511 (2008).
50. Tyanova, S. *et al.* The Perseus computational platform for comprehensive analysis of (prote)omics data. *Nat Methods* **13**, 731–740, doi:10.1038/nmeth.3901 (2016).
51. Livak, K. J. & Schmittgen, T. D. Analysis of relative gene expression data using real-time quantitative PCR and the 2(-Delta Delta C(T)) Method. *Methods* **25**, 402–408, doi:10.1006/meth.2001.1262 (2001).
52. Chen, P. *et al.* Modulation of gut mucosal microbiota as a mechanism of probiotics-based adjunctive therapy for ulcerative colitis. *Microb Biotechnol* **13**, 2032–2043, doi:10.1111/1751-7915.13661 (2020).
53. Mosher, J. J., Bernberg, E. L., Shevchenko, O., Kan, J. & Kaplan, L. A. Efficacy of a 3rd generation high-throughput sequencing platform for analyses of 16S rRNA genes from environmental samples. *J Microbiol Methods* **95**, 175–181, doi:10.1016/j.mimet.2013.08.009 (2013).
54. Edgar, R. C. Search and clustering orders of magnitude faster than BLAST. *Bioinformatics* **26**, 2460–2461, doi:10.1093/bioinformatics/btq461 (2010).
55. CoreTeam, R. R: A Language and Environment for Statistical Computing.. *R Foundation for Statistical Computing, Vienna.* (2013).
56. RStudioTeam. R Studio: Integrated Development for R. *Boston, MA:RStudio, Inc.* (2012).
57. pamr: Pam, prediction analysis for microarrays v. 1.56.1. (2018).
58. KA, L. C., González, I. & Déjean, S. integrOmics: an R package to unravel relationships between two omics datasets. *Bioinformatics* **25**, 2855–2856, doi:10.1093/bioinformatics/btp515 (2009).

Tables

Table 1. Proteins with differential abundance between the CON and ETEC pigs.

Accession number	Protein name	Gene name	Biological process	CON[a]	ETEC[a]	p	Effect Size
P10289	Gastrotropin	FABP6	bile acid transport	32.73 ± 0.35	31.65 ± 0.9	0.01[b]	1.46
P49924	Fatty acid-binding protein, liver	FABP1	fatty acid transport	28.59 ± 0.84	27.38 ± 0.91	0.03	1.28
F1SFL1	ADP ribosylation factor like GTPase 8B	ARL8B	antigen processing and presentation	24.77 ± 0.2	24.32 ± 0.17	0.01	2.20
A0A287BGN0	Cytochrome c oxidase subunit	COX6A1	energy metabolism	26.55 ± 0.35	25.88 ± 0.33	0.01	1.80
K7GNN0	Von Willebrand factor	VWF	immune response	23.97 ± 0.29	24.47 ± 0.24	0.01	-1.74
A0A287BTC2	DNA-(apurinic or apyrimidinic site) endonuclease	APEX1	nuclear acid metabolism	25.63 ± 0.17	26.08 ± 0.18	<0.01	-2.41
A0A5G2QGY8	Tubulointerstitial nephritis antigen like 1	TINAGL1	proteolysis	23.49 ± 0.47	24.2 ± 0.43	0.02	-1.44
F1SUH2	Cell division cycle and apoptosis regulator 1	CCAR1	cell cycle regulation	26.12 ± 0.45	26.83 ± 0.07	0.01[b]	-1.97
F1RIV0	2'-5'-oligoadenylate synthase-like protein isoform a	OASL	defense response to virus	24.34 ± 0.26	25.15 ± 0.57	0.05	-1.75

[a]Data are 2-based logarithm transformed and shown as mean ± SD; CON, no ETEC challenge; ETEC, ETEC challenge; P-values are calculated by Student's t test or [b]Wilcoxon rank-sum test.

Figures

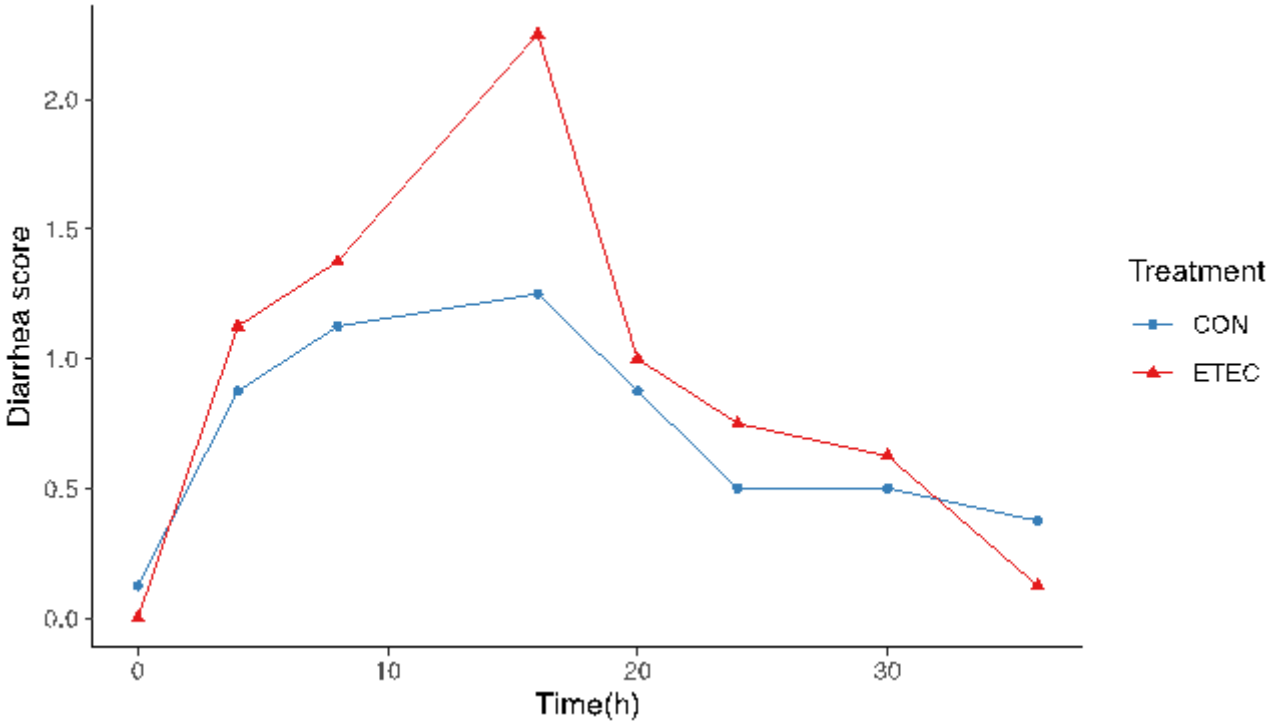

Figure 1

The diarrhea score over time post the ETEC challenge. 165 x 95 mm

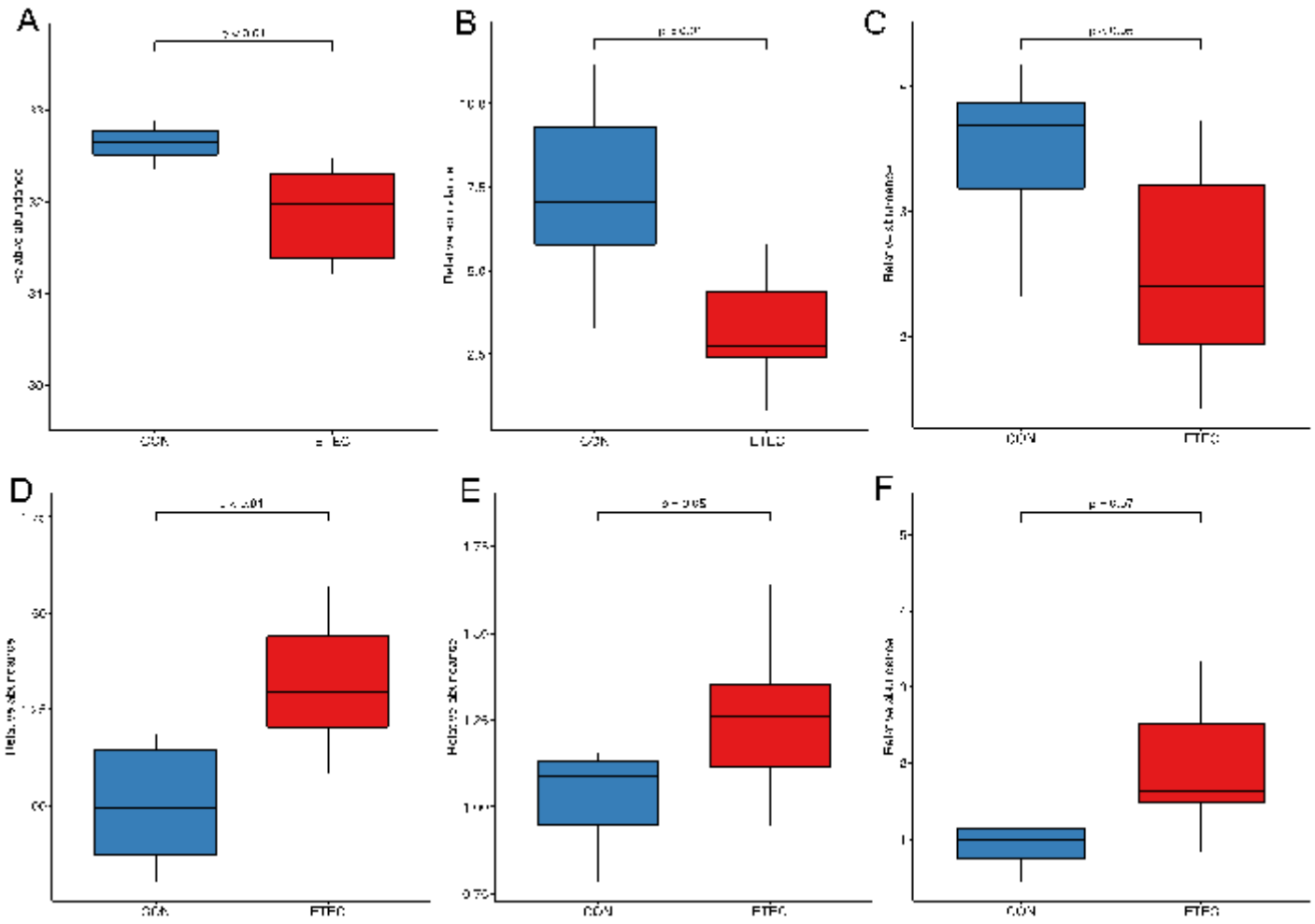

Figure 2

Relative abundance of FABP6 protein (A) and the transcription of selected genes ASBT (B), IL-18 (C), TLR9 (D), MyD88 (E), SIGIRR (F) in the ileum. 180 x 127 mm

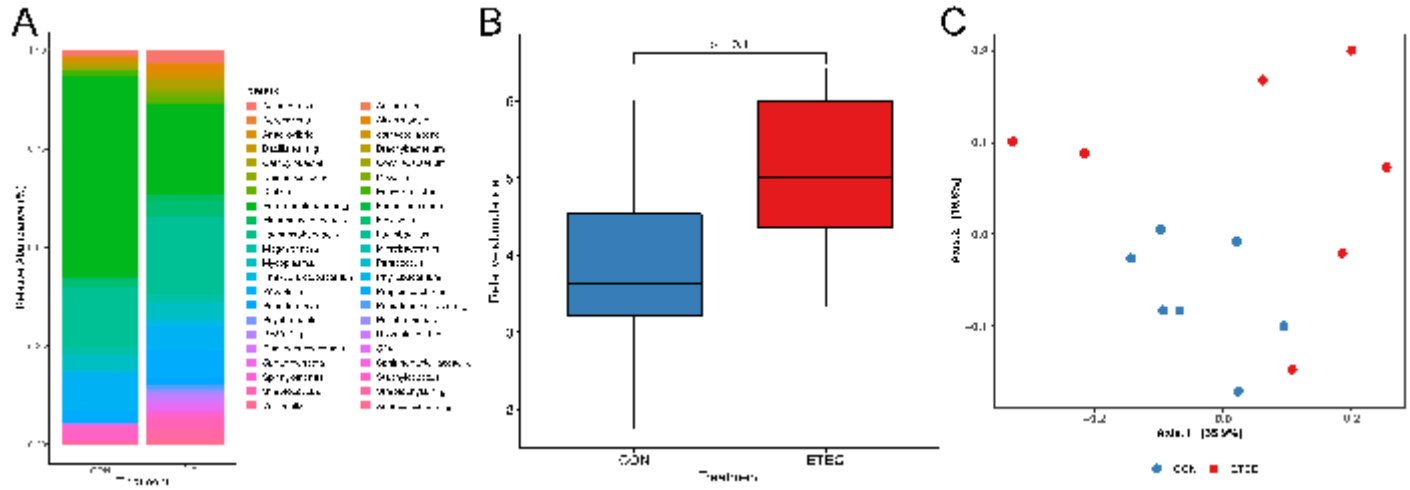

Figure 3

Relative richness plot (A), α-diversity (B) and β-diversity (unifrac dissimilarity, C) of ileal mucosa microbiome at the genus level. 180 x 64 mm

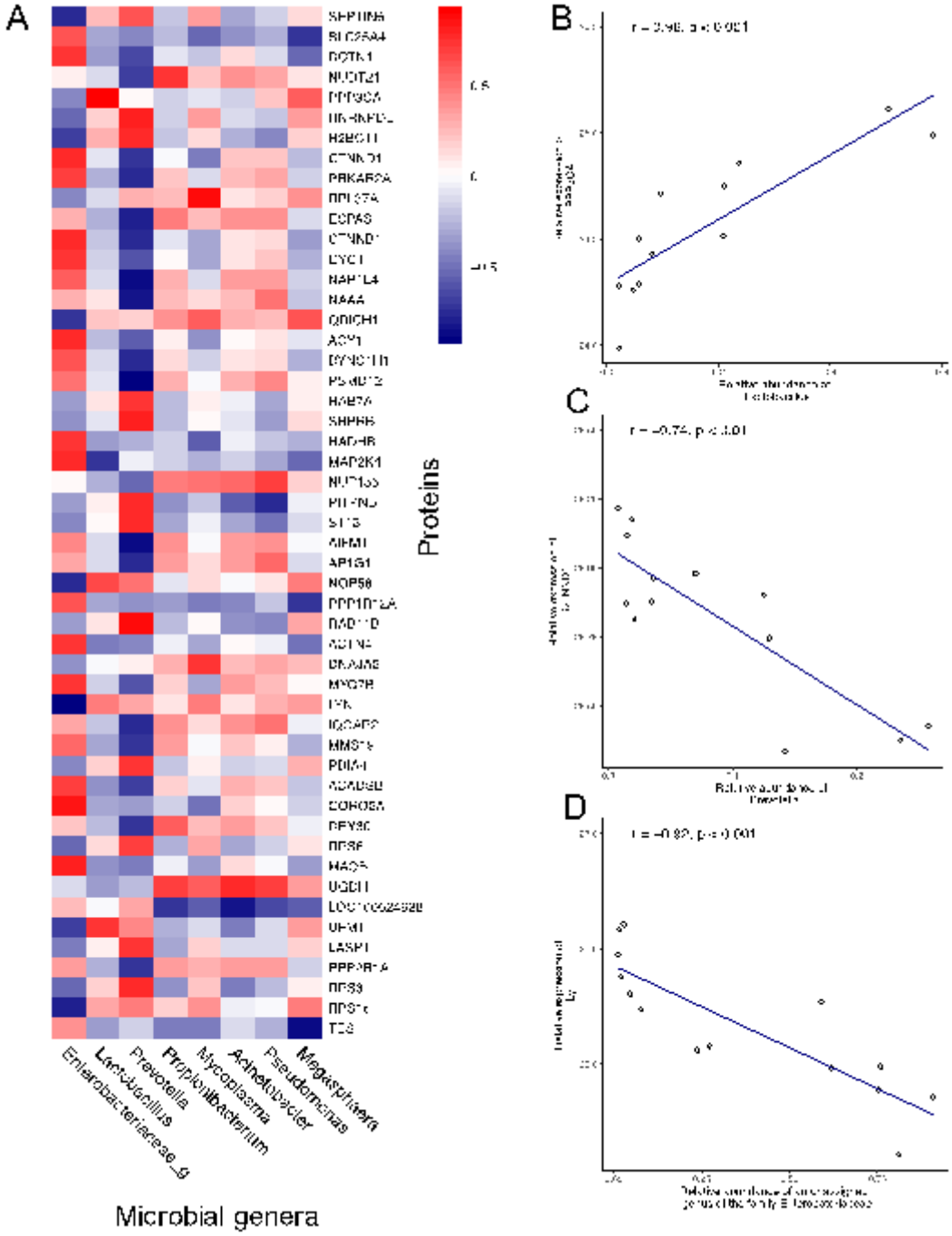

Figure 4

Heatmap showing the correlation between specific bacterial genera and mucosal proteins (A), scatter plots of the three key correlation pairs (B-D). 135 x 180 mm

Supplementary Files

This is a list of supplementary files associated with this preprint. Click to download.

- supplementaryfiles.docx